p66Shc deficiency enhances CXCR4 and CCR7 recycling in CLL B cells by facilitating their dephosphorylation-dependent release from Î²-arrestin at early endosomes

p66Shc deficiency enhances CXCR4 and CCR7 recycling in CLL B cells by facilitating their dephosphorylation-dependent release from β-arrestin at early endosomes

Laura Patrussi[1], Nagaja Capitani[1,2], Francesca Cattaneo[1], Noemi Manganaro[1], Alessandra Gamberucci[3], Federica Frezzato[4,5], Veronica Martini[4,5], Andrea Visentin[4,5], Pier Giuseppe Pelicci[6], Mario M D'Elios[2], Livio Trentin[4,5], Gianpietro Semenzato[4,5], Cosima T Baldari[1]

[1]Department of Life Sciences, University of Siena; [2]Department of Clinical and Experimental Medicine, University of Florence, Florence, Italy; [3]Department of Molecular and Developmental Medicine, University of Siena; [4]Venetian Institute of Molecular Medicine, Padua, Italy; [5]Department of Medicine, Hematology and Clinical Immunology Branch, Padua University School of Medicine, Padua, Italy; [6]European Institute of Oncology, Milan, Italy.

Equal contribution: LP and NC contributed equally to this work

Running title: p66Shc deficiency promotes CXCR4/CCR7 recycling in CLL

Keywords: CLL; receptor recycling; PP2B; chemokine; ibrutinib

Financial support: This work was carried out with the support of grant AIRC IG-15220 and ITT-Regione Toscana to CTB, AIRC IG-15286, Cariparo and Cariverona to GS and AIRC IG-15397 to LT.

Corresponding authors: Cosima T. Baldari, baldari@unisi.it, Via Aldo Moro 2, 53100 Siena, Italy. Tel: +39 0577 234400, Fax: +39 0577 234476; Laura Patrussi, patrussi2@unisi.it, Via Aldo Moro 2, 53100 Siena, Italy. Tel: +39 0577 234396, Fax: +39 0577 234476.

Conflict of interest: The authors declare no competing financial interests

Text word count: 4195

Figure count: 7

ABSTRACT

Neoplastic cell traffic abnormalities are central to the pathogenesis of chronic lymphocytic leukemia (CLL). Enhanced CXCR4 (CXC chemokine Receptor 4) and CCR7 (Chemokine Receptor 7) recycling contributes to the elevated surface levels of these receptors on CLL cells. Here we have addressed the role of p66Shc, a member of the Shc family of protein adaptors the expression of which is defective in CLL cells, in CXCR4/CCR7 recycling. p66Shc reconstitution in CLL cells reduced CXCR4/CCR7 recycling, lowering their surface levels and attenuating B-cell chemotaxis, due to their accumulation in $Rab5^{+}$ endosomes as serine-phosphoproteins bound to β-arrestin. This results from the ability of p66Shc to inhibit Ca^{2+} and PP2B-dependent CXCR4/CCR7 dephosphorylation and β-arrestin release. We also show that ibrutinib, a Btk inhibitor that promotes leukemic cell mobilization from lymphoid organs, reverses the CXCR4/CCR7 recycling abnormalities in CLL cells by increasing p66Shc expression. These results, identifying p66Shc as a regulator of CXCR4/CCR7 recycling in B cells, underscore the relevance of its deficiency to CLL pathogenesis and provide new clues to the mechanisms underlying the therapeutic effects of ibrutinib.

INTRODUCTION

The stromal microenvironment has emerged as a major player in the survival and expansion of neoplastic cell in chronic lymphocytic leukemia (CLL), a hematological neoplasm characterized by the progressive accumulation of mature $CD5^+$ B cells in blood, bone marrow (BM) and secondary lymphoid organs (SLO) (1-3). B lymphocyte homing to SLOs and BM is normally regulated by the chemokine receptors CCR7 (Chemokine Receptor 7) and CXCR4 (CXC chemokine Receptor 4), respectively, which respond to stroma-derived ligands (4-8). This activity is counteracted by sphingosine-1-phosphate (S1P) receptors that promote lymphocyte egress from their homing sites towards the S1P-rich circulatory fluids (9). CLL cells display abnormally high levels of surface CXCR4 and CCR7 (10-12) concomitant with a defect in S1PR1 (sphingosine-1-phosphate receptor 1) expression (13), resulting in an altered balance between entry and egress signals that might prolong leukemic cell residency in the pro-survival stromal niche.

The magnitude and duration of the cellular response to chemokines are regulated by receptor desensitization and resensitization, similar to other G protein-coupled receptors (GPCR). Ligand-bound GPCRs are phosphorylated by specific serine/threonine kinases and recruit β-arrestin, which induces their internalization and localization in $Rab5^+$ (Ras-related in brain 5) endosomes (14-18). The subsequent dephosphorylation allows receptor resensitization through recycling to the plasma membrane or alternatively their routing to lysosomes for degradation (16). The molecular machinery underlying CXCR4 and CCR7 dephosphorylation is unknown. CXCR4 and CCR7 recycling is potentiated in CLL cells, which accounts in part for their increased surface levels (11), underscoring the importance of characterizing this pathway.

We have implicated a defect of p66Shc, a proapoptotic Shc family member, in CLL pathogenesis (19). The impairment in p66Shc expression contributes to the apoptosis defects of CLL cells due to its ability to modulate the expression of Bcl-2 family genes (19). This activity extends to the genes encoding CCR7 and S1PR1, implicating p66Shc deficiency in the expression abnormalities of these receptors in CLL cells (13). Furthermore, p66Shc suppresses CXCR4 and CXCR5 signaling in normal B cells (20). Hence the p66Shc expression defect may impact at multiple levels on CLL cell trafficking to promote their accumulation in the stromal niche.

Here we asked whether p66Shc participates in the pathway that controls homing receptor recycling. We show that p66Shc is a negative regulator of CXCR4 and CCR7 recycling in B cells and that the enhanced ability of CLL cells to recycle these receptors is corrected by restoring p66Shc expression. We show that p66Shc limits CXCR4/CCR7 recycling by inhibiting their Ca^{2+} and PP2B (Phosphatase type 2B)-dependent dephosphorylation, on which their release from β-arrestin and transit to recycling endosomes was found to crucially depend. Furthermore, we provide evidence that ibrutinib, a Bruton tyrosine kinase (Btk) inhibitor used in combination therapies for CLL, normalizes the surface levels and subcellular distribution of CXCR4/CCR7 by limiting their recycling via an increase in p66Shc expression.

MATERIALS AND METHODS

Patients and healthy donors

Peripheral blood (PB) samples were collected from 49 patients satisfying standard morphologic and immunophenotypic criteria for CLL. B cells from 26 buffy coats were used as adult healthy population controls. At the time of collection, patients had never received treatment. For 5 patients, PB samples were collected before and after a 4-month Ibrutinib treatment with fixed daily dose of 420 mg, administered orally on continuous schedule.

B cells were purified by negative selection using RosetteSep B-cell enrichment Cocktail (StemCell Technologies, Vancouver, Canada) followed by density gradient centrifugation on Lympholite (Cedarlane Laboratories, The Netherlands).

Cell lines, plasmids, transfections and reagents

Stable control and p66Shc-expressing transfectants generated using the CLL-derived B-cell line MEC (21) were previously described (13,20). CLL cells were transiently cotransfected with 1 μg GFP reporter/sample and 5 μg pcDNA3 or the same vector encoding p66Shc (purified using the EndoFree Plasmid Maxi kit; Qiagen Gmbh, Hilden, Germany) using the Human B-cell Nucleofector Kit (Amaxa Biosystems, Cologne, Germany). Transfection efficiency was ≥40%, as assessed by flow cytometric analysis of GFP^+ cells, and cell viability 48 h post-transfection was 40-60%.

Reagents and antibodies are listed in the Supplemental Methods.

Mice

$p66Shc^{-/-}$/129 mice were previously described (22). Experiments were carried out on splenic B cells negatively purified by immunomagnetic sorting from age- and sex-matched 2-9-

month-old mice using the Dynabeads Mouse CD43 Negative Isolation Kit (Invitrogen srl, Leek, The Netherlands) (>85% purity).

Activations, immunoprecipitations and immunoblots

Cells were starved for 2 h in RPMI (Roswell Park Memorial Institute)-1% BSA and activated at 37°C with 500 ng/ml CXCL12 or 1 µg/ml CCL21 (Sigma-Aldrich). For immunoblots cells were lysed in 1% Triton X-100, 20 mM Tris-HCl (pH 8), 150 mM NaCl and protease inhibitors (Invitrogen). Post-nuclear supernatants were processed for immunoblot as described (23) or immunoprecipitated (2.5-5x10^7 cells/sample) using protein A-Sepharose (GE Healthcare).

RNA purification and RT-PCR

RNA was extracted and retrotranscribed as described (19). Real-time PCR was performed in triplicate on 96-well optical PCR plates (Sarstedt AG, Nümbrecht, Germany) using SSo Fast^{TM} EvaGreen^{R} SuperMix (Biorad Laboratories, Hercules, CA) and a CFX96 Real-Time system (Bio-Rad Laboratories, Waltham, MA). Results were processed and analyzed as described (11). Transcript levels were normalized to HPRT1. Primers used for amplification were previously described (11,13).

Analysis of receptor recycling, cell adhesion, chemotaxis and calcium flux

Flow cytometry was carried out using a Guava Easy Cyte (Millipore, Billerica, MA) cytometer. Analysis of surface CXCR4/CCR7 was carried out using fluorochrome-conjugated antibodies or isotype controls. To quantitate the ratio of surface to total CXCR4/CCR7, cells were fixed and permeabilized using the Cytofix/Cytoperm plus kit (BD Bioscience). CXCR4/CCR7 recycling following antibody-dependent downregulation was quantitated by flow cytometry as extensively described (24). Briefly, cells were incubated for

30 min on ice with receptor-specific Abs, washed, shifted to 37°C for 40 min, then subjected to acid stripping (time 0), and incubated for the indicated times at 37°C. Receptor:Ab complexes that had recycled to the cell surface were measured by labelling with fluorochrome-conjugated secondary antibodies. Before S1PR1 staining, cells were resuspended in serum-free medium, 0.5% fatty acid-free BSA (Sigma-Aldrich) and incubated for 30 min at 37°C to allow recycling of intracellular receptors. Adhesion assays on rhICAM-1/Fc (R&D Systems)- or Fibronectin (Sigma-Aldrich)-coated plates in the presence or absence of 100 ng/ml CXCL12/CCL21 were performed as described (20). Chemotaxis assays were carried out using 24-well Transwell chambers with 5-µm pore polycarbonate membranes (Corning Life Sciences, Schiphol-Rijk, The Netherlands) as described (23). Analysis of Ca^{2+} in Fura-2 loaded cells was carried out in 140 mM NaCl, 5.4 mM KCl, 1 mM $MgCl_2$, 0.2 mM EGTA, 15 mM Hepes, pH 7.4 in the absence of added Ca^{2+} as described (25).

Immunofluorescence microscopy, colocalization analyses and NF-AT assays

To analyze receptor recycling cells were equilibrated 30 min at 37°C in RPMI-1% BSA, incubated with 100 ng/ml CXCL12/CCL21 at 37°C for 10 or 40 min, permeabilized and processed for immunofluorescence microscopy as described (26). Images were acquired on a Zeiss LSM700 using a 63X objective as described (26). The quantitative colocalization analysis of CXCR4/CCR7 with β-arrestin or Rab was performed on median optical sections using ImageJ and JACoP plug-in to determine Manders' coefficient (27). For NF-AT assays, cells were transiently transfected with the plasmid pEGFP/NFAT-1D (28) using the Human B-cell Nucleofector Kit (primary B cells) or a modification of the DEAE/dextran procedure (MEC cells), as described (29). After 24 h, cells were resuspended in RPMI-1% BSA, stimulated with 100 ng/ml CXCL12/CCL21 at 37°C for 1 h or 500 ng/ml A23187 for 20 min, fixed and stained with anti-GFP antibodies.

Statistical analyses

Mean values, standard deviations and Student's *t* test (unpaired) were calculated using Microsoft Excel. The Mann-Whitney Rank Sum test was used to analyse CLL samples. A level of $p<0.05$ was considered statistically significant.

Study approval

Written informed consent was received from CLL patients and healthy donors prior to inclusion in the study according to the Declaration of Helsinki. Experiments were approved by the local Ethics Committee. All animal experiments were carried out in agreement with the Guiding Principles for Research Involving Animals and Human Beings and approved by the local ethics committee.

RESULTS

p66Shc negatively regulates CXCR4 and CCR7 recycling in B cells

Based on its ability to attenuate signaling by CXCR4 and CXCR5 (20), we investigated the impact of p66Shc expression on recycling of CXCR4 as well as of the related homing receptor CCR7, using as model the CLL-derived MEC B-cell line, which does not express p66Shc (13), stably transfected with a vector encoding this adaptor (p66) or with empty vector (ctr). Recycling to the plasma membrane of internalized CXCR4/CCR7 in cells treated with the respective specific antibodies was found to be profoundly impaired in the presence of p66Shc (Fig.1A and S1A). Similar results were obtained when CXCR4/CCR7 recycling was analyzed in splenic B cells purified from p66Shc$^{-/-}$ mice and their wild-type counterparts, where p66Shc is expressed at physiological levels (Fig.1B). A time course analysis of CXCR4/CCR7 downmodulation triggered by specific antibodies showed that p66Shc did not affect either the kinetics or the extent of receptor downmodulation (Fig.S1B,C). Hence p66Shc acts as a negative regulator of CXCR4 and CCR7 recycling downstream of their ligand-dependent internalization.

A substantial proportion of CXCR4/CCR7 is stored in recycling endosomes in B cells (11). We asked whether p66Shc may alter the quantitative balance between surface and vesicular CXCR4/CCR7 by interfering with their recycling. CXCR4/CCR7 were quantitated by flow cytometry in the intact and permeabilized MEC B-cell transfectants as well as on splenic B cells from wild-type and p66Shc$^{-/-}$ mice. The surface levels of CXCR4/CCR7 were found to be lower in the presence of p66Shc with a concomitant increase in the intracellular pool (Fig.S2A,B), resulting in a lower ratio of surface to total receptor in cells expressing

p66Shc (Fig.1C,D). Hence p66Shc affects the subcellular distribution of both receptors, favouring their association with the endosomal pool.

p66Shc reconstitution in CLL cells normalizes the chemokine-dependent enhancement in CXCR4/CCR7 recycling and chemotaxis

CXCR4/CCR7 recycling as well as the chemotactic responses elicited by these receptors are strongly enhanced in CLL cells, especially in patients with unmutated *IGHV* (Immunoglobulin Heavy chain Variable locus) (11). To assess whether the defect in p66Shc expression found in CLL cells (19) accounts for these recycling abnormalities, we measured CXCR4/CCR7 recycling in leukemic cells reconstituted with p66Shc (Fig.1E). Patients were grouped according to their *IGHV* mutational status (mutated, M-CLL; unmutated, U-CLL). Forced p66Shc expression resulted in a striking decrease in CXCR4/CCR7 recycling in both subgroups of patients (Fig.1E), implicating the p66Shc expression defect in the enhanced ability of CLL cells to recycle these receptors. p66Shc reconstitution in CLL cells also led to a modification in the subcellular distribution of CXCR4/CCR7, with a greater proportion of receptors that localized intracellularly to the expense of the plasma membrane compartment (Fig.S2C), resulting in a lower ratio of surface to total receptor (Fig.1F). Consistent with our previous reports (11,19), forced p66Shc expression in CLL cells resulted in a decrease in the mRNA and overall protein levels of CCR7 but did not affect the levels of CXCR4 (Fig.S3A,B). Hence, while the decreased amount of surface CCR7 in p66Shc-expressing B cells is in part related to its decreased expression levels, this does not apply to CXCR4, whose decrease can be fully accounted for by its reduced recycling.

Concomitant with the recycling-related reduction in surface CXCR4/CCR7 (Fig.S2C), p66Shc reconstitution in B cells from M-CLL and U-CLL patients resulted in a strong inhibition of CXCL12-/CCL21-dependent adhesion to both ICAM-1 (Fig.S4A) and Fibronectin (Fig.S4B) p66Shc reversed moreover the abnormally elevated migration of CLL cells towards CXCL12 and CCL21 (Fig.S4C,D). Hence, the p66Shc expression defect in CLL cells impinges on their responses to these chemokines at least in part by modulating the levels of the respective surface receptors through recycling.

p66Shc promotes the accumulation of internalized CXCR4/CCR7 in Rab5$^+$ endosomes as a complex with β-arrestin

To follow the fate of internalized CXCR4/CCR7, the MEC transfectants were stimulated with CXCL12/CCL21 to induce receptor internalization, then co-stained with antibodies to the respective receptors and for markers of early (Rab5) or recycling (Rab11) endosomes (11,17). As expected (11,17,18), both receptors co-localized to a significant extent with Rab11 (Fig.S5) and partially co-localized with Rab5 (Fig.2A) in the control transfectant. Forced p66Shc expression strongly enhanced the colocalization of recycling CXCR4/CCR7 with Rab5 (Fig.2A) while reducing their colocalization with Rab11 (Fig.S5). Interestingly, CXCL12/CCL21 readily triggered an association of Rab5 with both CXCR4 and CCR7 in the control transfectant which was lost at a later time of stimulation, as assessed by immunoprecipitation (Fig.3A). At variance with the transient interaction in ctr cells, the chemokine-dependent interaction of both receptors with Rab5 was sustained in the presence of p66Shc (Fig.3A). Hence internalized CXCR4/CCR7 rapidly transit through Rab5$^+$ endosomes to be sorted for recycling in MEC cells but accumulate in Rab5$^+$ endosomes in the presence of p66Shc, accounting for their impaired recycling.

GPCR internalization requires β-arrestin recruitment to serine-phosphorylated residue (14,15) which must be dephosphorylated for β-arrestin release and receptor recycling (30). Stabilization of the GPCR/β-arrestin complex is expected to prevent recycling. Imaging CXCR4/CCR7 in ctr MEC cells showed a strong but transient co-localization of both receptors with β-arrestin (Fig.2B) consistent with their recycling to the plasma membrane (Fig.1A), as opposed to the sustained co-localization at later times in p66Shc-expressing MEC cells (Fig.2B). Moreover the chemokine-triggered interaction of CXCR4/CCR7 with β-arrestin as well as Rab5 was found to be long-lasting in p66 cells when compared to ctr cells, as assessed by co-immunoprecipitation (Fig.3A). These data indicate that, in the presence of p66Shc, CXCR4/CCR7 internalized in response to ligand binding accumulate in association with β-arrestin in $Rab5^+$ vesicles and are therefore unable to transit to the $Rab11^+$ endosomes for recycling.

Both Rab5 and β-arrestin co-precipitated with p66Shc following stimulation with CXCL12/CCL21, forming a long-lasting complex (Fig.3B). Together with the ability of CXCR4/CCR7 to interact with p66Shc in a ligand-independent manner (Fig.3B), these data suggest that p66Shc may stabilize the association of these receptors with β-arrestin in early endosomes, preventing their further traffic along their recycling route.

To understand whether the p66Shc defect in CLL cells, which correlates with enhanced CXCR4/CCR7 recycling, leads to alterations in the dynamics of their interaction with Rab5 or β-arrestin similar to the MEC transfectants, we compared the colocalization of CXCR4/CCR7 with Rab5 and β-arrestin in B cells purified from healthy donors and M-CLL or U-CLL patients at a late time point of stimulation with the respective chemokines. A

significant colocalization of CXCR4/CCR7 with both Rab5 and β-arrestin was observed in B cells from healthy donors (Fig.4A,B) but was markedly lower in CLL cells (Fig.4A,B). Reconstitution of p66Shc in CLL cells largely restored the colocalization of CXCR4/CCR7 with Rab5 and β-arrestin (Fig.4C). Hence p66Shc deficiency leads to a reduction in CXCR4/CCR7 accumulation in early endosomes in CLL cells, accounting for their faster recycling.

p66Shc inhibits CXCR4 and CCR7 recycling by impairing their PP2B-dependent dephosphorylation

GPCRs traffic from $Rab5^+$ endosomes requires their dephosphorylation-dependent β-arrestin release (30). Since p66Shc impairs CXCR4/CCR7 recycling by promoting their accumulation in $Rab5^+$ endosomes in association with β-arrestin, we hypothesized that the dephosphorylation of these receptors might be impaired in the presence of p66Shc. CXCR4/CCR7 were immunoprecipitated from the MEC transfectants stimulated with the respective ligands at two different time points. Serine phosphorylation of both receptors was found to increase above basal levels in both ctr and p66Shc-expressing cells early after stimulation (Fig.5A). Interestingly, while CXCR4/CCR7 phosphorylation decreased at longer times in ctr cells, consistent with their re-exposure at the plasma membrane, it remained almost unchanged in p66Shc-expressing cells (Fig.5A). These data were confirmed by flow cytometric analysis for CXCR4 using a phosphospecific antibody (Fig.S6A). Consistent with the results obtained on the MEC transfectants, flow cytometric analysis showed that CXCR4 was transiently phosphorylated in response to CXCL12 in CLL cells as opposed to the sustained phosphorylation in primary B cells from healthy donors (Fig.S6B). This abnormality was reversed by forced p66Shc expression (Fig.S6C). Hence p66Shc prolongs

the interaction of CXCR4/CCR7 with β-arrestin and hence their residency in early endosomes by inhibiting their dephosphorylation.

The phosphoserine phosphatase responsible for CXCR4/CCR7 dephosphorylation is unknown. We reasoned that a pharmacological inhibitor that would phenocopy the effects of p66Shc expression would provide a clue to the identity of this phosphatase. CXCR4/CCR7 recycling was analyzed in ctr MEC cells pretreated with pharmacological inhibitors of phosphatases known to be implicated in recycling of other GPCRs. We used 10 nM Okadaic acid (OA) to inhibit PP2A (31), 100 nM OA to inhibit PP1 and PP2A (32), and 1 µM CsA or FK506 (Tacrolimus) to inhibit PP2B (33). Pharmacological inhibition of PP1 and PP2A did not affect CXCR4/CCR7 recycling. Conversely, a profound inhibition was observed in the presence of CsA or FK506 (Fig.5B), implicating PP2B in CXCR4 and CCR7 dephosphorylation. This notion was supported by the prolonged phosphorylation of CXCR4/CCR7 observed in receptor-specific immunoprecipitates of ctr MEC cells pretreated with CsA or FK506 and stimulated with the respective ligands at two different time points (Fig.5C).

Interestingly, PP2B was found to interact with both CXCR4 and CCR7 in the MEC transfectants, as assessed by co-immunoprecipitation. This interaction was enhanced in response to the respective chemokines early after stimulation in both transfectants (Fig.5D). While the amount of PP2B co-immunoprecipitated with CXCR4/CCR7 returned to basal levels at a longer stimulation time in ctr MEC cells, concomitant with their dephosphorylation (Fig.5A), this did not occur in p66-expressing cells (Fig.5D). These data support a role for PP2B in CXCR4/CCR7 dephosphorylation and suggest that PP2B is subsequently released to allow the receptors to recycle to the plasma membrane.

p66Shc inhibits CXCR4/CCR7-dependent PP2B activation by suppressing Ca^{2+} flux

To elucidate the mechanism underlying the inhibition of PP2B-dependent CXCR4/CCR7 dephosphorylation by p66Shc we tested the expression and activity of PP2B in the MEC transfectants. PP2B expression was not affected by p66Shc (Fig. 6A). Based on the Ca^{2+} dependence of PP2B (33) and the ability of p66Shc to attenuate CXCR4/CXCR5 signaling (20), we analyzed $[Ca^{2+}]_i$ mobilization in response to CXCL12/CCL21. Stimulation of ctr MEC cells with either chemokine triggered an elevation in $[Ca^{2+}]_i$ which was strongly impaired in the p66Shc-expressing transfectant (Fig.6B), suggesting that p66Shc may inhibit PP2B activation by blocking CXCR4/CCR7-dependent Ca^{2+} mobilization. To assess this possibility we transiently transfected ctr and p66Shc-expressing MEC cells with a reporter encoding GFP-tagged NFAT, a transcription factor which requires PP2B-mediated dephosphorylation to translocate to the nucleus (34), and scored the number of cells harbouring nuclear NFAT-GFP following stimulation with CXCL12 or CCL21. Both chemokines triggered nuclear translocation of NFAT-GFP in ctr MEC cells, which was impaired in the p66Shc-expressing transfectant (Fig. 6C). Of note, we did not observe any significant effect of p66Shc overexpression on chemokine-mediated apoptosis, as assessed by AnnexinV/PI staining, ruling out the possibility that p66Shc could impair cell viability, at least early after chemokine stimulation (Fig.S7). Hence p66Shc inhibits PP2B activation by impairing chemokine-dependent $[Ca^{2+}]_i$ mobilization, supporting the notion that the sustained phosphorylation of CXCR4/CCR7 in the presence of p66Shc results from defective PP2B activation.

Consistent with these results, B cells from CLL patients displayed an enhancement in CXCL12- and CCL21-dependent $[Ca^{2+}]_i$ mobilization (Fig.6E) and nuclear translocation of

NFAT-GFP (Fig.6F) compared to healthy donor B cells while expressing comparable levels of PP2B (Fig 6D). These data support the inhibitory role of p66Shc in PP2B-mediated dephosphorylation of CXCR4/CCR7 and provide a mechanism for the recycling defect in CLL cells.

Ibrutinib normalizes CXCR4 and CCR7 recycling by enhancing p66Shc expression

Treatment of CLL patients with ibrutinib, a Btk inhibitor used in clinical trials alone or in combination with conventional chemotherapeutic drugs (35,36), results in massive leukemic cell mobilization from lymph nodes paralleled by a transient lymphocytosis (37). We found that ibrutinib corrects the imbalance between homing and egress receptors in CLL cells *in vitro* and *in vivo* by modulating *CCR7* and *S1PR1* expression (11) (Fig.S8), which is expected to promote leukemic cell exit from the pro-survival stromal niche (37-40).

Since p66Shc modulates CCR7 and S1PR1 expression (13), we hypothesized that these effects of ibrutinib could be accounted for by enhanced p66Shc expression. Ibrutinib treatment of CLL cells resulted indeed in a robust dose-dependent increase in p66Shc expression, as measured by qRT-PCR (Fig.7A, S9A). Similar to the *in vitro* results, *in vivo* ibrutinib treatment resulted in a significant upregulation of p66Shc expression, as measured in CLL cells from patients administered daily for 4 months with ibrutinib (Fig.7A).

Consistent with the inhibitory effects of p66Shc on CXCR4/CCR7 recycling, ibrutinib-treated CLL cells displayed a reduction in CXCR4/CCR7 recycling (Fig.7B) and their subcellular distribution became largely intracellular (Fig.7C) resulting in a dose-dependent decrease in the ratio of surface to total receptors (Fig.7D, S9). Ibrutinib treatment restored moreover the

colocalization of CXCR4/CCR7 with Rab5 and β-arrestin in CLL cells (Fig.7E). These results further support a role for p66Shc as a central regulator of CXCR4/CCR7 transit throughout the recycling route.

DISCUSSION

Beside gene transcription (13), receptor recycling is an important determinant in controlling the levels of surface chemokine receptors and downstream responses in CLL (11). Here we implicate the p66Shc defect harboured by CLL cells (19) in the abnormal recycling on which elevated surface CXCR4/CCR7 expression largely depends. We show indeed that p66Shc negatively regulates CXCR4/CCR7 recycling by inhibiting the Ca^{2+}-dependent activation of the phosphatase PP2B that we identify as responsible for their dephosphorylation. This results in the accumulation of the internalized β-arrestin-bound receptors in $Rab5^+$ endosomes and hence their failure to transit to recycling endosomes. We provide moreover novel insights into the molecular mechanisms that underlie the therapeutic effects of ibrutinib in CLL by showing that it targets homing receptor recycling, normalizing the surface levels and subcellular distribution of CXCR4/CCR7 in CLL cells by upregulating p66Shc expression.

The cellular response to chemokines is rapidly modulated post-translationally by ligand-dependent receptor internalization and recycling. While little is known about CCR7, the mechanism regulating CXCR4 recycling has been partly elucidated in cell types other than B-lymphocytes, where it has been shown to require β-arrestin binding to the serine-phosphorylated cytosolic tail, internalization and transport to $Rab5^+$ endosomes (16-18,41-43). Similar to other GPCRs, β-arrestin release through dephosphorylation is expected to be essential for chemokine receptor transit from early to recycling endosomes (30,44). Our results show that this mechanism applies to CXCR4 and CCR7. Interestingly, while internalized CXCR4 is preferentially targeted to late endosomes and CCR7 to recycling endosomes in other cell types (16,17,45), these receptors appear to follow the same route in B cells, both undergoing recycling through a pathway involving dephosphorylation-

dependent β-arrestin release at early endosomes. Here we have identified PP2B as the phosphatase shared by CXCR4 and CCR7, with which it interacts, for this step.

p66Shc inhibits CXCR4- and CXCR5-dependent signaling by interacting with these receptors to promote the assembly of an inhibitory complex containing the phosphatases SHP-1 and SHIP-1, which results in impaired Syk (Spleen Tyrosine Kinase) and Btk phosphorylation (20). Both kinases contribute to BCR-dependent PLC-γ2 activation, which in turn initiates inositol-1,4,5-tris-phosphate-dependent $[Ca^{2+}]_i$ mobilization (46). Here we show a major defect of chemokine-dependent $[Ca^{2+}]_i$ mobilization in p66Shc-expressing B cells, which could be accounted for by impaired Syk and Btk phosphorylation. This defect is likely to underlie the defect in PP2B activation, which is dependent on Ca^{2+}-calmodulin, resulting in the failure of CXCR4/CCR7 to become dephosphorylated and hence in their endosomal accumulation.

Emerging evidence indicates that surface receptors continue signaling at endosomes following ligand-dependent internalization (47). This may compartmentalize signaling to specific functionally relevant subcellular localizations, as shown for endosomal β-2 adrenergic receptors (48). The finding that serine-phosphorylated CXCR4/CCR7 are found at $Rab5^+$ endosomes in association with β-arrestin and PP2B suggests that PP2B is activated locally to dephosphorylate the receptors, thereby allowing their transit to recycling endosomes. This could be achieved through $[Ca^{2+}]_i$ mobilization by endosomal CXCR4/CCR7. The tight packing of membrane compartments within the scant B-cell cytosol is expected to allow for $[Ca^{2+}]_i$ mobilization close to endosomes carrying signaling CXCR4/CCR7 from neighbouring endoplasmic reticulum cisternae and/or mitochondria. This process would be impaired in the presence of p66Shc due to its ability to interact with and inhibit Ca^{2+} signaling by endosomal CXCR4/CCR7.

The finding that p66Shc limits CXCR4/CCR7 recycling, together with its ability to modulate CCR7 and S1PR1 expression (13) and CXCR4 signaling (11), underscores the importance of the p66Shc defect in CLL cell homing to and accumulation in the protective stromal niche. This is supported by the rescue of p66Shc expression in ibrutinib-treated CLL cells, with the resulting inhibition of CXCR4/CCR7 recycling and decrease in their surface expression. These data provide a partial explanation for the molecular mechanisms that underlie the massive efflux of leukemic cells from lymphoid tissues and the consequent transient lymphocytosis in ibrutinib-treated patients (40,49). We have reported that p66Shc expression is regulated by the transcription factor STAT4, which is profoundly reduced in CLL cells (50), suggesting that ibrutinib may promote p66Shc expression by increasing the levels of STAT4.

In conclusion, we have identified p66Shc as a negative regulator of CXCR4/CCR7 recycling acting at the early-to-recycling endosome transit step by preventing their Ca^{2+}-dependent dephosphorylation by receptor-associated PP2B. We have moreover implicated the p66Shc defect in CLL cells in the recycling abnormalities of CXCR4 and CCR7, which contribute to their robust responses to the respective pro-survival stromal ligands. Finally, we provide new insights into the mechanisms underlying the therapeutic effects of ibrutinib in CLL**.**

Acknowledgements

The authors wish to thank Sonia Grassini for technical assistance. This work was carried out with the support of grant AIRC IG-15220 and ITT-Regione Toscana to CTB, AIRC IG-15286, Cariparo and Cariverona to GS and AIRC IG-15397 to LT.

REFERENCES

1. Scarfo L, Ferreri AJ, Ghia P. Chronic lymphocytic leukaemia. *Crit Rev Oncol Hematol.* **2016**;104:169-82.

2. Burger JA, Gribben JG. The microenvironment in chronic lymphocytic leukemia (CLL) and other B cell malignancies: insight into disease biology and new targeted therapies. *Semin Cancer Biol.* **2014**;24:71-81.

3. Munk Pedersen I, Reed J. Microenvironmental interactions and survival of CLL B-cells. *Leuk Lymphoma.* **2004**;45:2365-72.

4. Kehrl JH, Hwang IY, Park C. Chemoattract receptor signaling and its role in lymphocyte motility and trafficking. *Curr Top Microbiol Immunol.* **2009**;334:107-27.

5. Kucia M, Jankowski K, Reca R, Wysoczynski M, Bandura L, Allendorf DJ, et al. CXCR4-SDF-1 signalling, locomotion, chemotaxis and adhesion. *J Mol Histol.* **2004**;35:233-45.

6. Comerford I, Harata-Lee Y, Bunting MD, Gregor C, Kara EE, McColl SR. A myriad of functions and complex regulation of the CCR7/CCL19/CCL21 chemokine axis in the adaptive immune system. *Cytokine Growth Factor Rev.* **2013**;24:269-83.

7. Kurtova AV, Balakrishnan K, Chen R, Ding W, Schnabl S, Quiroga MP, *et al.* Diverse marrow stromal cells protect CLL cells from spontaneous and drug-induced apoptosis: development of a reliable and reproducible system to assess stromal cell adhesion-mediated drug resistance. *Blood.* **2009**;114:4441-50.

8. Ten Hacken E, Burger JA. Microenvironment interactions and B-cell receptor signaling in Chronic Lymphocytic Leukemia: Implications for disease pathogenesis and treatment. *Biochim Biophys Acta.* **2016**;1863:401-13.

9. Jin L, Liu WR, Tian MX, Fan J, Shi YH. The SphKs/S1P/S1PR1 axis in immunity and cancer: more ore to be mined. *World J Surg Oncol.* **2016**;14:131.

10. Redondo-Munoz J, Jose Terol M, Garcia-Marco JA, Garcia-Pardo A. Matrix metalloproteinase-9 is up-regulated by CCL21/CCR7 interaction via extracellular signal-regulated kinase-1/2 signaling and is involved in CCL21-driven B-cell chronic lymphocytic leukemia cell invasion and migration. *Blood.* **2008**;111:383-6.

11. Patrussi L, Capitani N, Martini V, Pizzi M, Trimarco V, Frezzato F, *et al.* Enhanced Chemokine Receptor Recycling and Impaired S1P1 Expression Promote Leukemic Cell Infiltration of Lymph Nodes in Chronic Lymphocytic Leukemia. *Cancer Res.* **2015**;75:4153-63.

12. López-Giral S, Quintana NE, Cabrerizo M, Alfonso-Pérez M, Sala-Valdés M, De Soria VG, *et al.* Chemokine receptors that mediate B cell homing to secondary lymphoid tissues are highly expressed in B cell chronic lymphocytic leukemia and non-Hodgkin lymphomas with widespread nodular dissemination. *J Leukoc Biol.* **2004**;76:462-71.

13. Capitani N, Patrussi L, Trentin L, Lucherini OM, Cannizzaro E, Migliaccio E, *et al.* S1P1 expression is controlled by the pro-oxidant activity of p66Shc and is impaired in B-CLL patients with unfavorable prognosis. *Blood.* **2012**;120:4391-9.

14. Kang DS, Tian X, Benovic JL. Role of beta-arrestins and arrestin domain-containing proteins in G protein-coupled receptor trafficking. *Curr Opin Cell Biol.* **2014**;27:63-71.

15. Gurevich VV, Gurevich EV. Arrestins: Critical Players in Trafficking of Many GPCRs. *Prog Mol Biol Transl Sci.* **2015**;132:1-14.

16. Marchese A. Endocytic trafficking of chemokine receptors. *Curr Opin Cell Biol.* **2014**;27:72-7.

17. Otero C, Groettrup M, Legler DF. Opposite fate of endocytosed CCR7 and its ligands: recycling versus degradation. *J Immunol.* **2006**;177:2314-23.

18. Zhang Y, Foudi A, Geay JF, Berthebaud M, Buet D, Jarrier P, *et al.* Intracellular localization and constitutive endocytosis of CXCR4 in human CD34+ hematopoietic progenitor cells. *Stem Cells.* **2004**;22:1015-29.

19. Capitani N, Lucherini OM, Sozzi E, Ferro M, Giommoni N, Finetti F, *et al.* Impaired expression of p66Shc, a novel regulator of B-cell survival, in chronic lymphocytic leukemia. *Blood*. **2010**;115:3726-36.

20. Patrussi L, Capitani N, Cannizzaro E, Finetti F, Lucherini OM, Pelicci PG, *et al.* Negative regulation of chemokine receptor signaling and B-cell chemotaxis by p66Shc. *Cell Death Dis.* **2014**;5:e1068.

21. Stacchini A, Aragno M, Vallario A, Alfarano A, Circosta P, Gottardi D, *et al.* MEC1 and MEC2: two new cell lines derived from B-chronic lymphocytic leukaemia in prolymphocytoid transformation. *Leuk Res.* **1999**;23:127-36.

22. Migliaccio E, Giorgio M, Mele S, Pelicci G, Reboldi P, Pandolfi PP, *et al.* The p66shc adaptor protein controls oxidative stress response and life span in mammals. *Nature*. **1999**;402:309-13.

23. Patrussi L, Ulivieri C, Lucherini OM, Paccani SR, Gamberucci A, Lanfrancone L, *et al.* p52Shc is required for CXCR4-dependent signaling and chemotaxis in T cells. *Blood*. **2007**;110:1730-8.

24. Patrussi L, Baldari CT. Analysis of TCR/CD3 Recycling at the Immune Synapse. *Methods Mol Biol.* **2017**;1584:143-55.

25. Gamberucci A, Giunti R, Benedetti A. Progesterone inhibits capacitative Ca2+ entry in Jurkat T lymphocytes by a membrane delimited mechanism, independently of plasma membrane depolarization. *Cell Calcium.* **2004**;36:175-80.

26. Finetti F, Paccani SR, Riparbelli MG, et al. Intraflagellar transport is required for polarized recycling of the TCR/CD3 complex to the immune synapse. *Nat Cell Biol.* **2009**;11:1332-9.

27. Manders EM, Stap J, Brakenhoff GJ, van Driel R, Aten JA. Dynamics of three-dimensional replication patterns during the S-phase, analysed by double labelling of DNA and confocal microscopy. *J Cell Sci.* **1992**;103:857-62.

28. Plyte S, Boncristiano M, Fattori E, Galvagni F, Paccani SR, Majolini MB, *et al.* Identification and characterization of a novel nuclear factor of activated T-cells-1 isoform expressed in mouse brain. *J Biol Chem.* **2001**;276:14350-8.

29. Boncristiano M, Paccani SR, Barone S, Ulivieri C, Patrussi L, Ilver D, *et al.* The Helicobacter pylori vacuolating toxin inhibits T cell activation by two independent mechanisms. *J Exp Med.* **2003**;198:1887-97.

30. Vasudevan NT, Mohan ML, Goswami SK, Naga Prasad SV. Regulation of beta-adrenergic receptor function: an emphasis on receptor resensitization. *Cell Cycle.* **2011**;10:3684-91.

31. Swingle M, Ni L, Honkanen RE. Small-molecule inhibitors of ser/thr protein phosphatases: specificity, use and common forms of abuse. *Methods Mol Biol.* **2007**;365:23-38.

32. Martinez-Martinez S, Redondo JM. Inhibitors of the calcineurin/NFAT pathway. *Curr Med Chem.* **2004**;11:997-1007.

33. Schulz RA, Yutzey KE. Calcineurin signaling and NFAT activation in cardiovascular and skeletal muscle development. *Dev Biol.* **2004**;266:1-16.

34. Serfling E, Berberich-Siebelt F, Chuvpilo S, Jankevics E, Klein-Hessling S, Twardzik T, *et al.* The role of NF-AT transcription factors in T cell activation and differentiation. *Biochim Biophys Acta.* **2000**;1498:1-18.

35. Burger JA, Tedeschi A, Barr PM, Robak T, Owen C, Ghia P, *et al.* Ibrutinib as Initial Therapy for Patients with Chronic Lymphocytic Leukemia. *N Engl J Med.* **2015**;373:2425-37.

36. Lee CS, Rattu MA, Kim SS. A review of a novel, Bruton's tyrosine kinase inhibitor, ibrutinib. *J Oncol Pharm Pract.* **2016**;22:92-104.

37. Byrd JC, Furman RR, Coutre SE, Flinn IW, Burger JA, Blum KA, *et al.* Targeting BTK with ibrutinib in relapsed chronic lymphocytic leukemia. *N Engl J Med.* **2013**;369:32-42.

38. Cheng S, Ma J, Guo A, Lu P, Leonard JP, Coleman M, *et al.* BTK inhibition targets in vivo CLL proliferation through its effects on B-cell receptor signaling activity. *Leukemia.* **2014**;28:649-57.

39. Wodarz D, Garg N, Komarova NL, Benjamini O, Keating MJ, Wierda WG, *et al.* Kinetics of CLL cells in tissues and blood during therapy with the BTK inhibitor ibrutinib. *Blood.* **2014**;123:4132-5.

40. de Rooij MF, Kuil A, Geest CR, Eldering E, Chang BY, Buggy JJ, *et al.* The clinically active BTK inhibitor PCI-32765 targets B-cell receptor- and chemokine-controlled adhesion and migration in chronic lymphocytic leukemia. *Blood.* **2012**;119:2590-4.

41. Charest-Morin X, Pepin R, Gagne-Henley A, Morissette G, Lodge R, Marceau F. C-C chemokine receptor-7 mediated endocytosis of antibody cargoes into intact cells. *Front Pharmacol.* **2013**;4:122.

42. Lagane B, Chow KY, Balabanian K, Levoye A, Harriague J, Planchenault T, *et al.* CXCR4 dimerization and beta-arrestin-mediated signaling account for the enhanced chemotaxis to CXCL12 in WHIM syndrome. *Blood*. **2008**;112:34-44.

43. Bamidele AO, Kremer KN, Hirsova P, Clift IC, Gores GJ, Billadeau DD, *et al.* IQGAP1 promotes CXCR4 chemokine receptor function and trafficking via EEA-1+ endosomes. *J Cell Biol.* **2015**;210:257-72.

44. Kennedy JE, Marchese A. Regulation of GPCR Trafficking by Ubiquitin. *Prog Mol Biol Transl Sci.* **2015**;132:15-38.

45. Berlin I, Higginbotham KM, Dise RS, Sierra MI, Nash PD. The deubiquitinating enzyme USP8 promotes trafficking and degradation of the chemokine receptor 4 at the sorting endosome. *J Biol Chem.* **2010**;285:37895-908.

46. Wienands J. The B-cell antigen receptor: formation of signaling complexes and the function of adaptor proteins. *Curr Top Microbiol Immunol.* **2000**;245:53-76.

47. Calebiro D, Nikolaev VO, Persani L, Lohse MJ. Signaling by internalized G-protein-coupled receptors. *Trends Pharmacol Sci.* **2010**;31:221-8.

48. Bowman SL, Shiwarski DJ, Puthenveedu MA. Distinct G protein-coupled receptor recycling pathways allow spatial control of downstream G protein signaling. *J Cell Biol.* **2016**;214:797-806.

49. Herman SE, Mustafa RZ, Jones J, Wong DH, Farooqui M, Wiestner A. Treatment with Ibrutinib Inhibits BTK- and VLA-4-Dependent Adhesion of Chronic Lymphocytic Leukemia Cells In Vivo. *Clin Cancer Res.* **2015**;21:4642-51.

50. Cattaneo F, Patrussi L, Capitani N, Frezzato F, D'Elios MM, Trentin L, *et al.* Expression of the p66Shc protein adaptor is regulated by the activator of transcription STAT4 in normal and chronic lymphocytic leukemia B cells. *Oncotarget.* **2016**; 7:57086-98.

FIGURES AND LEGENDS

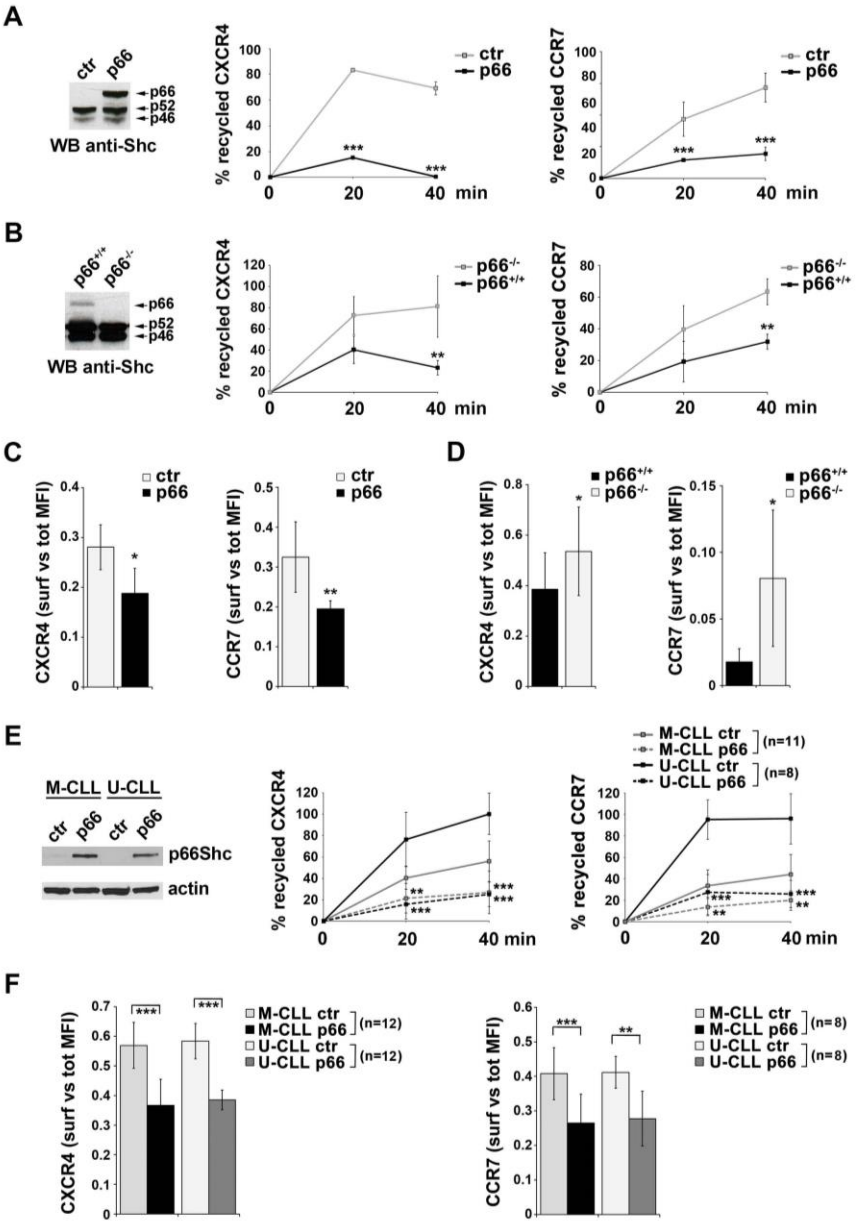

Figure 1. p66Shc negatively regulates CXCR4 and CCR7 recycling in B cells. A, B. Flow cytometric analysis of CXCR4/CCR7 recycling in MEC B cells stably transfected with empty vector (ctr) or with a vector encoding p66Shc (p66) (**A**), or in splenic B cells purified from wild-type ($p66^{+/+}$) or p66Shc$^{-/-}$ ($p66^{-/-}$) mice (**B**). Data are presented as % of internalized receptors that have recycled to the cell surface at the indicated times and refer to duplicate samples from 4 independent experiments (**A**) or to duplicate samples from 8 $p66^{+/+}$ and 8 $p66^{-/-}$ mice (**B**). The immunoblot analysis with anti-Shc antibodies of postnuclear supernatants from ctr and p66 MEC B cells (**A**) or from purified splenic B cells from 8 wild-

type and 8 p66Shc$^{-/-}$ mice (**B**) are shown on the left of the respective panels. **C, D.** Ratio of surface to total MFI of CXCR4 and CCR7 in ctr and p66 MEC B cells (**C,** n≥4), or in splenic B cells purified from p66$^{+/+}$ or p66$^{-/-}$ mice (**D,** duplicate samples from 8 wild-type and 8 p66Shc$^{-/-}$ mice). Data are expressed as ratio (mean±SD) of MFI in non-permeabilized cells (surface) to permeabilized (total) cells. **E.** Flow cytometric analysis of CXCR4/CCR7 recycling in purified M-CLL or U-CLL B cells nucleofected with either empty vector (ctr) or an expression construct encoding p66Shc (p66). Data are presented as % of internalized receptors that have recycled to the cell surface at the indicated times and refer to duplicate samples for each patient. The immunoblot analysis with anti-Shc and anti-actin antibodies of postnuclear supernatants from the CLL transfectants is shown on the left. **F.** Ratio of surface to total MFI of CXCR4 (left) and CCR7 (right) from M-CLL or U-CLL ctr or p66Shc B cell transfectants. Data are expressed as ratio (mean±SD) of MFI in non-permeabilized cells (surface) to permeabilized (total) cells. Error bars, SD. Student's *t* test (unpaired). $p<0.001$, ***; $p<0.01$, **; $p<0.05$, *.

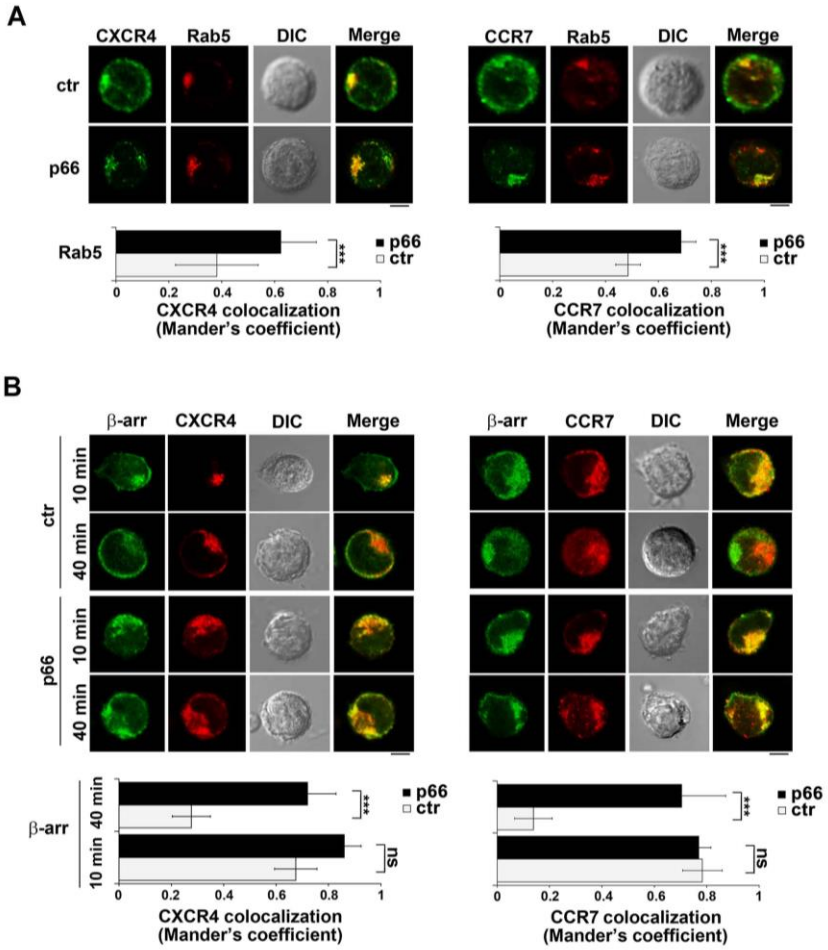

Figure 2. p66Shc expression enhances CXCR4/CCR7 colocalization with Rab5 and β-arrestin in MEC B cells. A. Immunofluorescence analysis of Rab5 (red) and either CXCR4 (green, *left*) or CCR7 (green, *right*) in ctr and p66 MEC B cells incubated with 100 ng/ml of CXCL12/CCL21 at 37°C for 40 min, fixed and permeabilized. Representative median optical sections are shown. The quantification using Mander's coefficient of the weighted colocalization of CXCR4 (left) or CCR7 (right) with Rab5 in individual medial confocal sections is shown below the corresponding images (n=3). **B.** Immunofluorescence analysis of β-arrestin (green) and either CXCR4 (red, *left*) or CCR7 (red, *right*) in ctr and p66 MEC B cells incubated with 100 ng/ml of CXCL12/CCL21 at 37°C for either 10 or 40 min, fixed and permeabilized. Representative median optical sections are shown. The quantification using Mander's coefficient of the weighted colocalization of CXCR4 (left) or CCR7 (right) with β-arrestin in individual medial confocal sections is shown below the corresponding images (n=3). Representative median optical sections are shown. Size bar, 5 μm, mean±SD; ≥20 cells/marker. Error bars, SD. Student's *t* test (unpaired). $p<0.001$, ***.

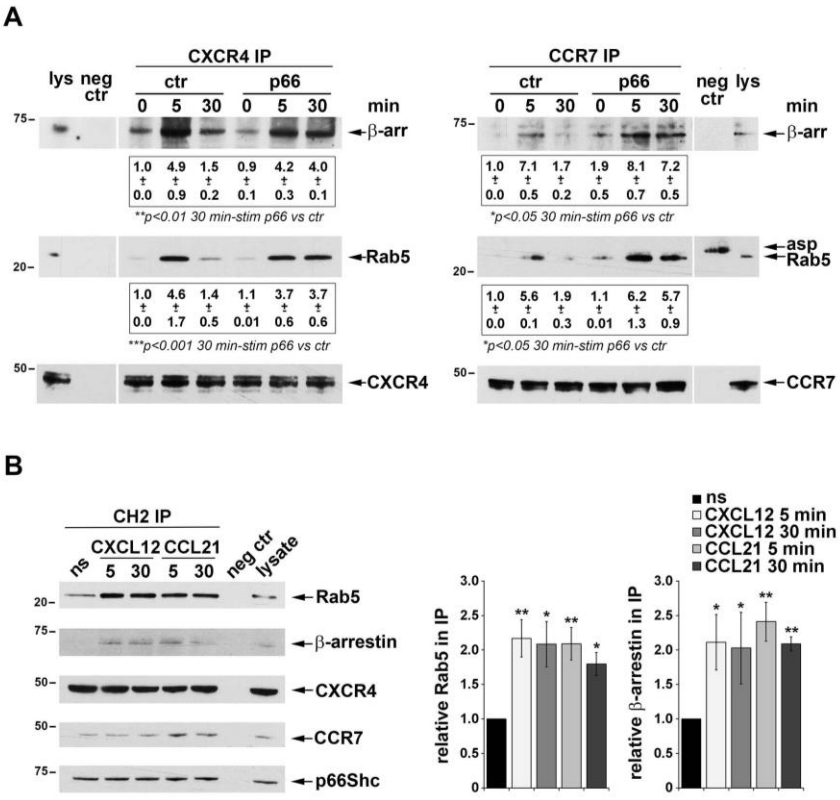

Figure 3. p66Shc stabilizes the interaction of CXCR4/CCR7 with Rab5 and β-arrestin in MEC B cells. A. Immunoblot analysis with anti-β-arrestin and anti-Rab5 antibodies of CXCR4- (left) and CCR7- (right) specific immunoprecipitates from lysates of ctr and p66 MEC B cells, either unstimulated or activated with either 500 ng/ml CXCL12 or 1 µg/ml CCL21. The stripped filters were reprobed with anti-CXCR4 or anti-CCR7 antibodies. The quantification of the relative amount of β-arrestin and Rab5 is indicated below the respective immunoblots. **B**. Immunoblot analysis with anti- β-arrestin, -Rab5, -CXCR4 and -CCR7 antibodies of CH2-specific immunoprecipitates from lysates of p66 MEC B cells, either unstimulated or activated with either 500 ng/ml CXCL12 or 1 µg/ml CCL21. The stripped filters were reprobed with anti-Shc antibodies. The quantification of the relative amount of Rab5 and β-arrestin co-immunoprecipitated with p66Shc is shown on the right. The migration of molecular mass markers is indicated. The immunoblots shown in the figure are representative of 3 independent experiments. Error bars, SD. Student's *t* test (unpaired). $p<0.01$, **; $p<0.05$, *.

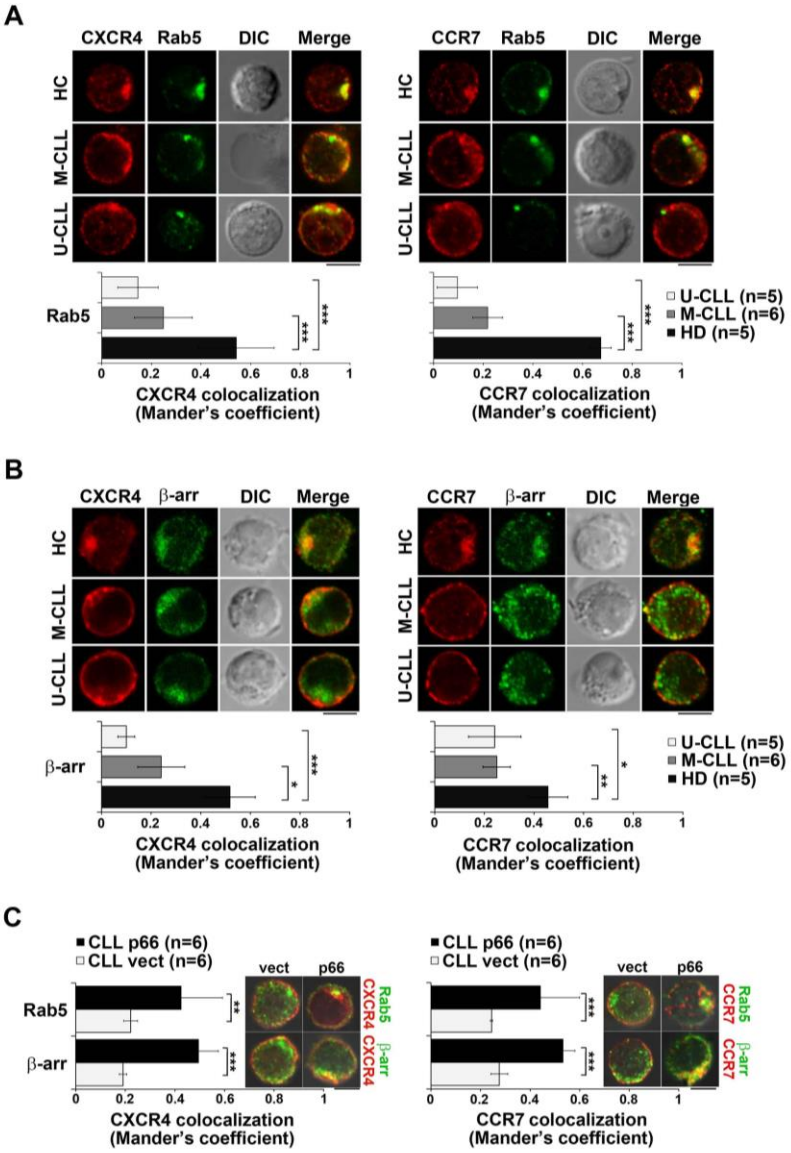

Figure 4. p66Shc reconstitution in CLL B cells enhances CXCR4/CCR7 colocalization with Rab5 and β-arrestin. A.B. Immunofluorescence analysis of Rab5 (red, upper panel) (**A**) or β-arrestin (red, lower panel) (**B**), and either CXCR4 (green) or CCR7 (green) in purified healthy control (HC), M-CLL or U-CLL B cells incubated with 100 ng/ml of CXCL12/CCL21 at 37°C for 40 min, fixed and permeabilized. Size bar, 5 µm. The quantification using Mander's coefficient of the weighted colocalization of CXCR4 (left) or CCR7 (right) with Rab5 and β-arrestin in individual medial confocal sections is shown below the corresponding images. **C**. Quantification using Mander's coefficient of the weighted colocalization of CXCR4 (left) or CCR7 (right) with Rab5 and β-arrestin in individual medial confocal sections of purified M-CLL or U-CLL B cells, nucleofected with either empty vector (ctr) or an expression construct encoding p66Shc (p66), incubated with 100 ng/ml of CXCL12/CCL21 at 37°C for 40 min, fixed and permeabilized (mean±SD; ≥20 cells/marker). Representative median optical sections are shown. Size bar, 5 µm. Error bars, SD. Mann-Whitney Rank Sum test (unpaired). $p<0.001$, ***; $p<0.01$, **; $p<0.05$, *.

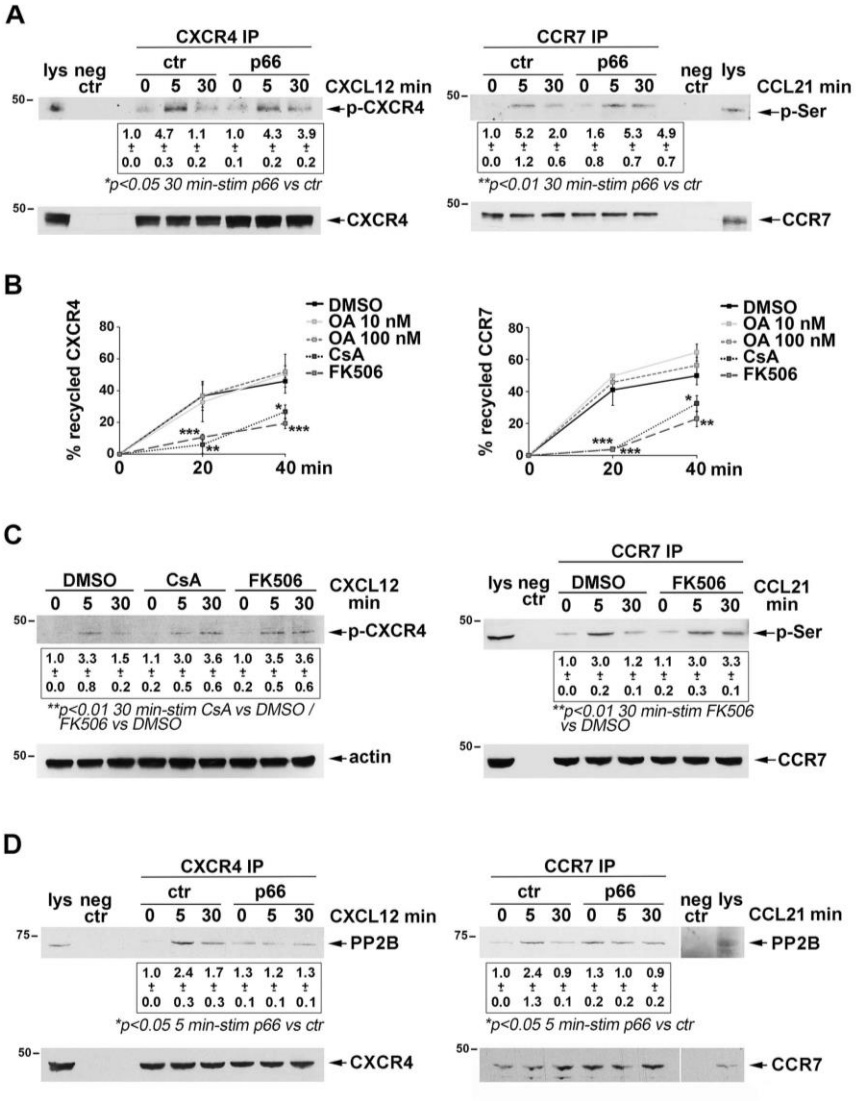

Figure 5. p66Shc inhibits PP2B-dependent dephosphorylation of CXCR4 and CCR7. **A.** Immunoblot analysis with anti- phospho-CXCR4 or anti -phospho-Serine antibodies of either CXCR4- (left) or CCR7- (right) specific immunoprecipitates from lysates of ctr and p66 MEC B cells, either unstimulated or activated for 5 and 30 min with either 500 ng/ml CXCL12 or 1 µg/ml CCL21. The stripped filters were reprobed with anti-CXCR4 or anti-CCR7 antibodies. **B**. Flow cytometric analysis of CXCR4/CCR7 recycling in MEC B cells stably transfected with empty vector (ctr) or with a vector encoding p66Shc (p66), incubated for 30 min at 37°C with either DMSO, 10 and 100 nM okadaic acid, 1 µM CsA or 1 µM FK506. Data are presented as % of internalized receptors that have recycled to the cell surface at the indicated times and refer to duplicate samples from 3 independent experiments. **C**. Immunoblot analysis with anti- phospho-CXCR4 or anti-phospho-Serine antibodies of either CXCR4- (left) or CCR7- (right) specific immunoprecipitates from lysates of ctr MEC B cells, incubated for 30 min at 37°C with either DMSO or 1 µM CsA and either unstimulated or activated for 5 and 30 min with either 500 ng/ml CXCL12 or 1 µg/ml CCL21. The stripped filters were reprobed with anti-CXCR4 or anti-CCR7 antibodies. **D**. Immunoblot analysis with anti- PP2B antibodies of either CXCR4- (left) or CCR7- (right) specific immunoprecipitates

from lysates of ctr and p66 MEC B cells, either unstimulated or activated for 5 and 30 min with either 500 ng/ml CXCL12 or 1 µg/ml CCL21. The stripped filters were reprobed with anti-CXCR4 or anti-CCR7 antibodies. The quantification of the relative protein amount is indicated below the respective immunoblots. The immunoblots shown in the figure are representative of 3 independent experiments. Error bars, SD. Student's *t* test (unpaired). $p<0.001$, ***; $p<0.01$, **; $p<0.05$, *.

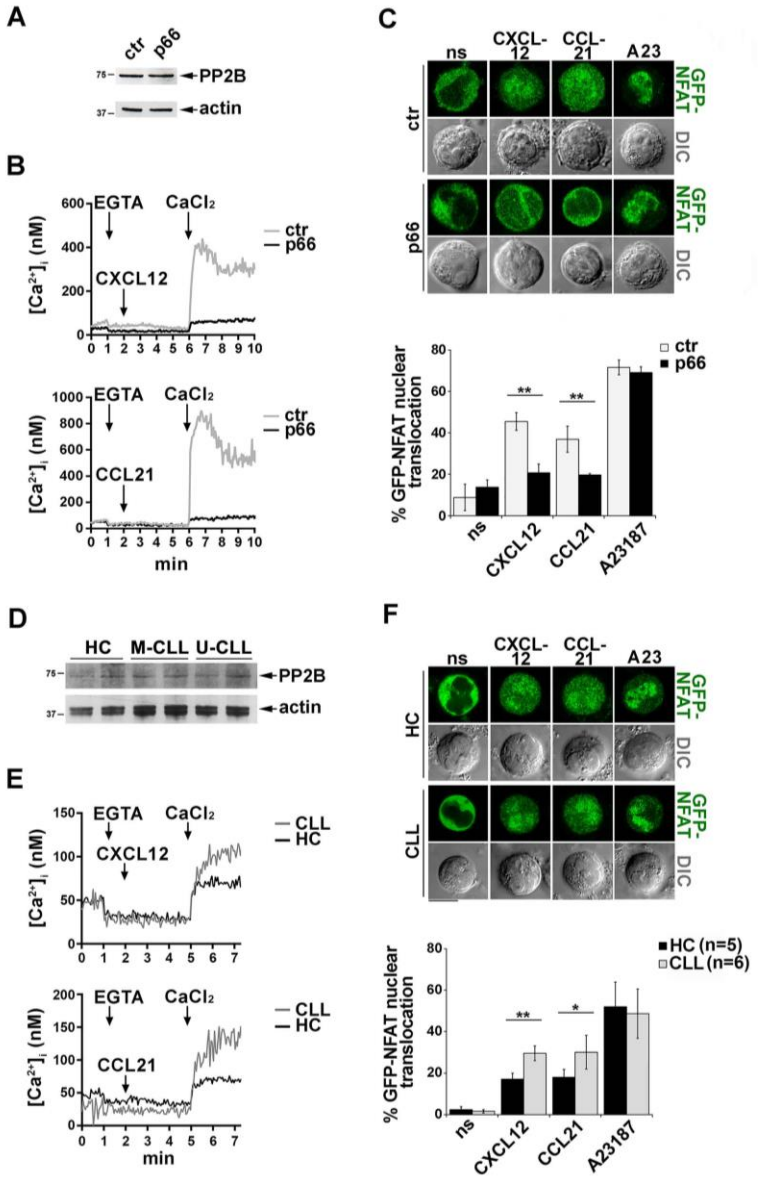

Figure 6. p66Shc inhibits CXCR4/CCR7-dependent PP2B activation. A, D. Immunoblot analysis with anti-PP2B antibodies of postnuclear supernatants from ctr and p66 MEC B cells (**A**) or from purified healthy control (HC), M-CLL or U-CLL B cells (**D**). The stripped filters were reprobed with anti-actin antibodies. **B.** Fluorimetric analysis of $[Ca^{2+}]_i$ in ctr and p66 MEC B cells stimulated with 100 ng/ml of CXCL12/CCL21. The arrow indicates the time of addition of chemokines, 1 mM EGTA and 1 mM $CaCl_2$, respectively. The total levels of store-associated Ca^{2+}, as measured after cell solubilization by digitonin treatment in the presence of EGTA, were similar in all cell lines. Representative experiments are shown (n=3). **C**. Confocal microscopy of ctr and p66 MEC B cells transiently transfected with a GFP-NFAT expression construct, either unstimulated (ns) or stimulated with 100 ng/ml CXCL12 or CCL21 for 1 h or with 500 ng/ml A23187 (A23) for 20 min. The percentage of cells displaying nuclear GFP-NFAT was calculated by analyzing at least 100 cells/sample (n=3). **E.** Fluorimetric analysis of $[Ca^{2+}]_i$ in purified HC or CLL B cells stimulated with 100

ng/ml CXCL12 or CCL21. The total levels of store-associated Ca^{2+} were similar in all samples (not shown). Representative experiments are shown (HC=4, CLL=3). The average area under curve (AUC) of CXCL12-stimulated Ca^{2+} influx was 78+/-14.7 for CLL, 35.6+/-15.3 for HC samples; the average AUC of CCL21-stimulated Ca^{2+} influx was 106.4+/-44 for CLL, 54+/-4.222 for HC samples. **F**. Confocal microscopy of purified HC or CLL B cells transiently transfected with a GFP-NFAT expression construct, either unstimulated (ns) or stimulated with 100 ng/ml of CXCL12 or CCL21 for 1 h or with 500 ng/ml A23 for 20 min. The percentage of cells displaying nuclear GFP-NFAT was calculated by analyzing at least 100 cells/sample (HC=5, M-CLL=6). Error bars, SD. Student's *t* test (unpaired). $p<0.01$, **; $p<0.05$, *.

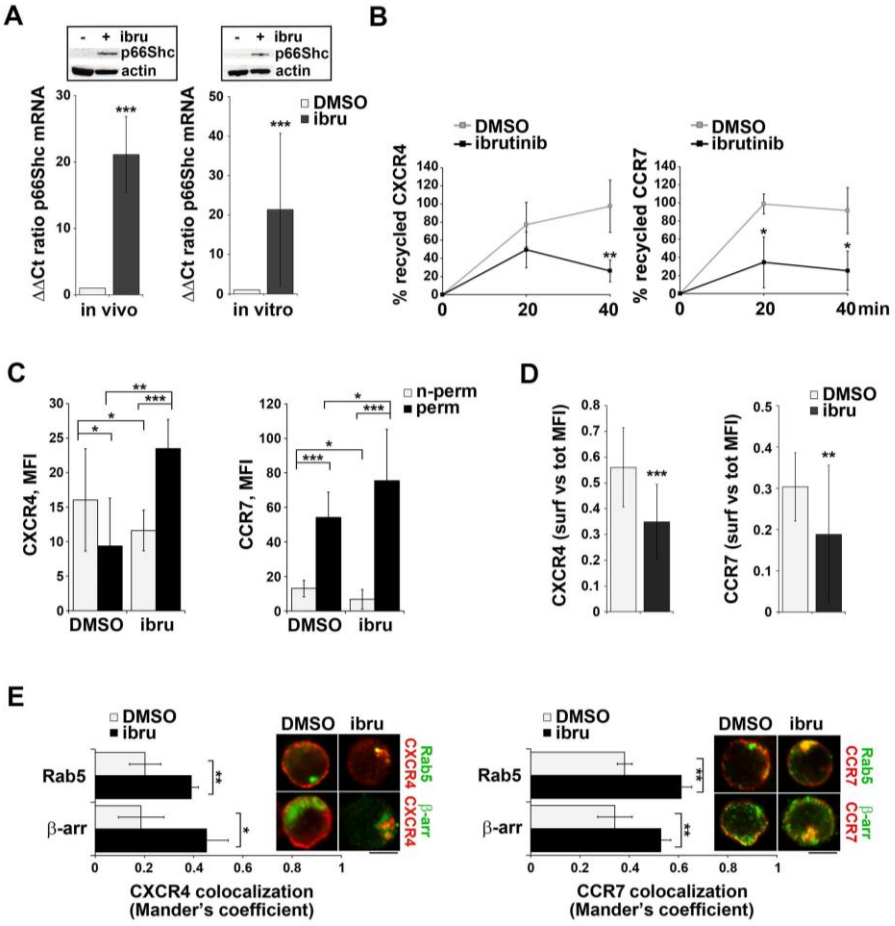

Figure 7. Ibrutinib promotes p66Shc expression in CLL cells and normalizes CXCR4 and CCR7 recycling. A. *Bottom*, Quantitative RT-PCR analysis of p66Shc mRNA on purified peripheral B cells from either 5 CLL patients with lymphadenopathy, before (pre) and after (post) 4-month in vivo ibrutinib treatment, or 23 CLL patients treated in vitro with either DMSO or 10 μM ibrutinib for 48 h. The relative gene transcript abundance was determined on triplicate samples using the ddCt method (fold change in samples post- versus pre-treatment). *Top*, immunoblot analysis with anti-Shc antibodies of CLL cells treated or untreated with ibrutinib, as above. The stripped filter was reprobed with anti-actin antibodies. **B**. Flow cytometric analysis of CXCR4/CCR7 recycling in purified CLL B cells treated in vitro with either DMSO or 10 μM ibrutinib for 48 h. Data are presented as % of internalized receptors that have recycled to the cell surface and refer to duplicate samples (n=4). **C**. Flow cytometric analysis of CXCR4 or CCR7 on purified CLL B cells treated in vitro with either DMSO or 10 μM ibrutinib for 48 h, either non-permeabilized (n-perm) or permeabilized (perm). **D.** Ratio of surface to total MFI of CXCR4 and CCR7 from CLL B cells treated in vitro with either DMSO or 10 μM ibrutinib for 48 h. Data are expressed as ratio of MFI in non-permeabilized cells (surface) to permeabilized (total) cells. **E.** Quantification using Mander's coefficient of the weighted colocalization of CXCR4 or CCR7 with Rab5 and β-arrestin in individual medial confocal sections of purified CLL B cells treated in vitro with either DMSO or 10 μM ibrutinib for 48 h, incubated with 100 ng/ml of CXCL12/CCL21 at 37°C for 40 min, fixed and permeabilized. Representative median optical sections are shown on the right (mean±SD; ≥20 cells/marker). Size bar, 5 μm. Error bars, SD. Mann-Whitney Rank Sum test (unpaired). $p<0.001$, ***; $p<0.01$, **; $p<0.05$, *.